New Phytologist

Low temperature reduces the energetic requirement for the CO_2 concentrating mechanism in diatoms

Sven A. Kranz[1,4], Jodi N. Young[1], Brian M. Hopkinson[2], Johanna A. L. Goldman[1], Philippe D. Tortell[3] and François M. M. Morel[1]

[1]Department of Geosciences, Princeton University, Princeton, NJ 08544, USA; [2]Department of Marine Science, University of Georgia, Athens, GA 30602, USA; [3]Department of Earth, Ocean and Atmospheric Sciences, University of British Columbia, Vancouver, BC V6T 1Z4, Canada; [4]Present address: Department of Earth, Ocean and Atmospheric Sciences, Florida State University, Tallahassee, FL 32306, USA

Author for correspondence:
Sven A. Kranz
Tel: +1 609 258 2489
Email: skranz@princeton.edu

Received: *19 May 2014*
Accepted: *1 July 2014*

New Phytologist (2015) **205:** 192–201
doi: 10.1111/nph.12976

Key words: CO_2 concentrating mechanism, diatoms, modeling, phytoplankton, primary production, psychrophilic, Western Antarctic Peninsula.

Summary

- The goal of this study is to investigate the CO_2 concentrating mechanism (CCM) of the dominant phytoplankton species during the growing season at Palmer station in the Western Antarctic Peninsula.
- Key CCM parameters (cellular half-saturation constants for CO_2 fixation, carbonic anhydrase activity, CO_2/HCO_3^- uptake, $\delta^{13}C_{org}$) in natural phytoplankton assemblages were determined. Those results, together with additional measurements on CO_2 membrane permeability from *Fragilariopsis cylindrus* laboratory cultures, were used to develop a numerical model of the CCM of cold water diatoms.
- The field data demonstrate that the dominant species throughout the season possess an effective CCM, which achieves near saturation of CO_2 for fixation. The model provides a means to examine the role of eCA activity and HCO_3^-/CO_2 uptake in the functioning of the CCM. According to the model, the increase in $\delta^{13}C_{org}$ during the bloom results chiefly from decreasing ambient CO_2 concentration (which reduces the gross diffusive flux across the membrane) rather than a shift in inorganic carbon uptake from CO_2 to HCO_3^-.
- The CCM of diatoms in the Western Antarctic Peninsula functions with a relatively small expenditure of energy, resulting chiefly from the low half-saturation constant for Rubisco at cold temperatures.

Introduction

High-latitude regions are among the most productive in the world oceans (Arrigo *et al.*, 2008b). In particular, the intense phytoplankton blooms common in the spring on the continental shelf regions of Antarctica result in a high degree of CO_2 sequestration through biological carbon fixation (Holm-Hansen *et al.*, 1989; Smetacek *et al.*, 1992; Sullivan *et al.*, 1993; Arrigo *et al.*, 2008a,b). The concentration of CO_2 in the polar surface oceans is generally high as a result of the increase in CO_2 solubility with decreasing temperature: atmosphere equilibrated CO_2 concentration is *c.* 25 μM at 0°C compared to 13 μM at 20°C (Zeebe & Wolf-Gladrow, 2007). This high CO_2 concentration should facilitate inorganic carbon acquisition and alleviate the demand for a CO_2 concentrating mechanism (CCM) utilized by phytoplankton to overcome the poor affinity of Rubisco for CO_2 (Badger *et al.*, 1998; Giordano *et al.*, 2005). However, during phytoplankton blooms, the CO_2 can become undersaturated (Sweeney, 2003) and this effect is amplified by the low buffering capacity of high-latitude seawater (Egleston *et al.*, 2010). At those times, the reduced diffusion rate of CO_2 in cold water (a factor of 2 between 0 and 20°C; Boudreau, 1997) may limit its rate of supply to phytoplankton. The slow turnover rate of Rubisco at low temperature can exacerbate this problem (Dutkiewicz *et al.*, 2009; Young *et al.*, 2014). The poor CO_2 buffering capacity, the slow diffusion of CO_2 and the slow enzymatic carboxylation rate may make the operation of the CCM particularly critical during phytoplankton blooms in cold water.

A number of field studies at high latitudes, particularly in the Ross and Weddell Seas, provide context for our work (Cassar *et al.*, 2004; Tortell *et al.*, 2008a,b, 2010, 2013; Neven *et al.*, 2011). The publications reported measurements of HCO_3^- vs CO_2 uptake and extracellular carbonic anhydrase (eCA) activity by the ambient population. Most importantly they demonstrated that the carbon fixation by the ambient flora was nearly CO_2 saturated (Tortell *et al.*, 2010), thus implying the presence of an active CCM in the dominant phytoplankton species. Laboratory studies have demonstrated effective CCMs in a variety of psychrophilic diatoms, although important differences between species were seen in eCA activity and ratios of HCO_3^- and CO_2 uptake (Mitchell & Beardall, 1996; Trimborn *et al.*, 2013).

Here we extend the available data on the CCM of phytoplankton assemblages of the Southern Ocean to the high-productivity shelf region. We report on a seasonal study at Palmer Station in the Western Antarctic Peninsula (WAP) where we measured the extent of CO_2 saturation of the ambient phytoplankton

population during the development of a massive spring bloom in 2012/2013. We complemented the field data with laboratory experiments using the well-studied Antarctic diatom species, *Fragilariopsis cylindrus*, to constrain some of the key parameters necessary for developing a numerical model of the CCM of an idealized psychrophilic diatom. We used this model to quantify the cellular and sub-cellular fluxes of inorganic carbon and to examine the energetic costs of the CCM in diatoms at low temperatures.

Materials and Methods

Field sampling procedure

Samples were collected between the end of October and end of March at the Palmer Station Long Term Ecological Research site (station B; Latitude: −64.7795; Longitude: −64.0725), along the Western Antarctic Peninsula. A Monsoon Pump (Waterra WSP-SS-80-NC; Waterra Pumps Ltd, Mississauga, ON, Canada) was used to collect water from a 10-m depth into various sample containers (cleaned with 2 M HCl and washed with MilliQ and sample-site seawater). Water for carbonate chemistry analysis was collected into a 4-l Polycarbonate bottle and closed without headspace. Water for the physiological measurements of the phytoplankton community (half-saturation constants for CO_2 ($K_{1/2}$), HCO_3^-/CO_2 uptake ratios, and eCA measurements) was dispensed into translucent 20-l carboys.

Cells for HCO_3^-/CO_2 uptake ratios, eCA activity and cellular carbon kinetics ($K_{1/2}$) were immediately concentrated via inline pressure filtration. An aquarium pump (Aqua-Supreme Air Pump 2; Danner Manufacturing Inc., Islandia, NY, USA) was connected to a polypropylene carboy and the seawater was pushed through a 2-μm polycarbonate filter (EMD Millipore). The filter was subsequently transferred into method-specific buffers where cells were gently removed off the filter. During filtration, as is customary, cells were kept under laboratory light (low light) for 2–3 h. For HCO_3^-/CO_2 uptake ratios and cellular carbon kinetics, cells were allowed to acclimate for 15–30 min at a 200 μmol photons m^{-2} s^{-1} light intensity before experiments were conducted.

Carbonate chemistry

Samples for total alkalinity (TA) were filtered through 0.2-μm syringe filters (Whatman; GE Healthcare, Piscataway, NJ, USA), collected in 200-ml borosilicate bottles, spiked with 5 μl of saturated mercury chloride and stored at 2°C in the dark. Measurements were conducted (*c.* 3–9 months after collection) by potentiometric titration (Brewer *et al.*, 1986) with an average precision of ± 7 μmol kg^{-1}. TA was calculated from linear Gran Plots (Gran, 1952) and measurements were calibrated using certified reference seawater standards (supplied by Dr Andrew Dickson, Scripps Institution of Oceanography).

Seawater pH was determined by potentiometry until mid-December and spectrophotometrically afterwards (Zhang & Byrne, 1996). For the potentiometric measurement, the electrode was two-point calibrated on ice every day and samples were measured on ice, with temperature probe compensation. For the spectrophotometric method, 10 μl Thymol blue (2 mM) was added to 1 ml of seawater. The sample was measured using a Cary 4000 UV-VIS-NIR spectrophotometer (Varian, Palo Alto, CA, USA) after temperature equilibration to 20–22°C. Conversion and temperature correction of the pH measurement to a seawater pH scale was done using CO2sys (Lewis & Wallace, 1998). The two different pH determination methods were compared and found to be well correlated (slope = 1.004, $R^2 = 0.98$, $n = 81$). The carbonate system was calculated from TA, pH, temperature, salinity, phosphate and silicate using CO2Sys. Equilibrium constants where those of Mehrbach *et al.* (1973) as refitted by Dickson & Millero (1987). Carbonate chemistry is given in Supporting Information Table S1.

Chl*a* and $\delta^{13}C_{org}$

Cells were collected onto GF/F filters and immediately transferred to 5 ml 90% acetone for Chl*a* extraction (18–24 h at −20°C). Chl*a* concentration was determined with a fluorometer (Turner Designs 10-AU; Sunnyvale, CA, USA) by measuring nonacidified and acidified fluorescence (Welschmeyer, 1994). The fluorometer was calibrated at the beginning of the season using pure Chl*a* extract from spinach (Sigma-Aldrich). $\delta^{13}C$ from the suspended particulate material ($\delta^{13}C_{org}$) in the WAP was measured by filtering 100–500 ml water onto 25 mm GF/F (pre-combusted at 500°C for 9 h) which were acidified by fumigation with 6 N HCl overnight and dried at 60°C for 2 d. Samples were measured using Elemental Combustion Analyzer (Costech, Valencia, CA, USA) coupled to an Isotope Ratio Mass Spectrometer (DeltaV Advantage; Thermo Scientific, Waltham, MA, USA) and calibrated against the standard reference material, peach leaf (NIST 2157; Becker, 1990).

Cellular carbon fixation kinetics

Carbon fixation kinetics of WAP phytoplankton assemblages as well as *F. cylindrus* cultures were determined by measuring ^{14}C fixation for 10–15 min over a range of inorganic carbon concentrations (Tortell *et al.*, 2010). Before measurement, cells were re-suspended in CO_2 free buffer (pH 8.0; HEPES 50 μM), and various amounts of ^{14}C-HCO_3^- were added. Carbon uptake was terminated by the addition of 50% HCl to samples (see Tortell *et al.* (2010) for full experimental details). Data were fitted with a Michaelis–Menten hyperbolic equation to derive least-squares estimates for half-saturation constants ($K_{1/2}$).

Carbonic anhydrase

The activity of extracellular carbonic anhydrase, eCA, was measured in WAP phytoplankton assemblages and *F. cylindrus* cultures by following ^{18}O exchange between CO_2 and HCO_3^- according to Silverman (1982). A Pfeiffer Quadrupole Mass Spectrometer (Pfeiffer Vacuum, Asslar, Germany) connected to a temperature-controlled chamber via a gas permeable membrane

(PTFE, 0.01 mm thick) was used for these measurements. eCA assays were carried out in the dark by re-suspending concentrated cells into 8 ml of 0.2-μm filtered seawater buffered with HEPES (50 mM, pH 8.0) at 2°C. The method uses the depletion of ^{18}O from aqueous $^{13}C^{18}O_2$ caused by the hydration and dehydration steps of CO_2 and HCO_3^- (Fig. S1). For comparison with rates of CO_2 diffusive flux to the cell surface, additional estimates of the eCA activity per cell, based on the same technique, were made according to Hopkinson *et al.* (2013). A more detailed method description can be found in the Methods S1.

Internal CA activity was estimated from the rapid decline in log (enrichment) upon the injection of cells and calculated according to Hopkinson *et al.* (2011) (Methods S1).

^{14}C disequilibrium method (HCO_3^-/CO_2 uptake ratio)

The ^{14}C-disequilibrium technique makes use of the transient isotopic disequilibrium upon the addition of an acidic ^{14}C spike into cell suspension at high pH to determine the relative amount of CO_2 or HCO_3^- taken up by cells to support photosynthesis (Espie & Colman, 1986; Elzenga *et al.*, 2000). In the present study we followed the protocol described by Martin & Tortell (2006) and Rost *et al.* (2007). Cells were re-suspended into buffered seawater (bicine-NaOH; 20 mM; pH 8.5; 2.5°C) and transferred into a cuvette (3-ml volume). After pre-incubation to 200 μmol photons m^{-2} s^{-1} for 15 min, 200 μl of $H^{14}CO_3^-$ (in MilliQ; 50 mM HEPES; pH 7.0) was added and sub-samples were taken over the duration of 15 min. External CA activity was inhibited by the use of dextran-bound sulfonamide (DBS; 50 μM). Data were fitted according to Rost *et al.* (2007),with constants calculated for 2.5°C, to derive estimates of $fHCO_3^-$ (i.e. fraction of C uptake attributable to HCO_3^- transport).

Data from cultures of *Fragilariopsis cylindrus*

Fragilariopsis cylindrus (CCMP 1102), an abundant psychrophilic diatom, was grown in a semi-continuous, dilute batch culture using 0.2-μm filtered coastal seawater (obtained from the Institute of Marine and Coastal Science (IMCS) at Rutgers University (USA)) supplemented with Aquil macro- and micro- nutrients (Sunda *et al.*, 2005) under continuous light (150 μmol photons m^{-2} s^{-1}) at 0.5°C. Cultures were acclimated to these conditions for at least 4 wk. Cells were kept between 20 000 and 700 000 cells ml^{-1}, monitored with a Coulter Counter Z2 (Beckman Coulter Inc., Fullerton, CA, USA). Regular dilution (every *c.* 10 d) ensured that cells were in exponential growth phase. Growth was determined by counting cells daily over an 8-d period. To keep carbonate chemistry constant, cultures were continuously sparged with air containing 400 μatm CO_2, generated using a gas flow controller (Fideris TesSol Inc., Battle Ground, WA, USA) in which CO_2 free air (< 1 ppmv CO_2, CO_2 free air generator; Parker Domnick Hunter, Fairfield, OH, USA) was mixed with pure CO_2 (Air Liquide, Houston, TX, USA). The CO_2 concentration of the gas was continuously monitored using an infrared gas analyzer (LI-840A; Li-Cor, Lincoln, NE, USA). For measurements, cells were concentrated by gentle filtration (2 μm; Polycarbonate filter) down to a volume of *c.* 5 ml and rinsed twice with 50 ml of assay buffer. Cells were allowed to acclimate to 200 μmol photons m^{-2} s^{-1} before experiments (^{14}C disequilibrium assay, cellular carbon kinetics) were conducted. Cells for membrane permeability determination and eCA activity were kept in the dark during the assay.

Numerical model

We developed a generic CCM model for psychrophilic diatoms based on the existing model of Hopkinson *et al.* (2011, 2013) to quantify the fluxes of inorganic carbon species in and out of cellular compartments. Data obtained at Palmer station from the diatoms during the bloom (cell size, $\delta^{13}C_{org}$, HCO_3^-/CO_2 uptake, eCA activity, Rubisco concentration (Young *et al.*, 2014)) as well as data obtained in the laboratory with *F. cylindrus* (membrane diffusivity for CO_2 and HCO_3^-, internal CA activity and Rubisco kinetics; Young *et al.*, 2014) were used to constrain model parameters (Table S2).

In the model, HCO_3^- transport into the cytoplasm and chloroplast are the only active fluxes and are described by Michaelis–Menten kinetics. CO_2 fluxes between compartments are passive and parameterized using mass transfer coefficients. For the cytoplasmic membrane, these mass transfer coefficients were measured for the psychrophilic diatom *F. cylindrus* following the protocol described in Hopkinson *et al.* (2011). For the chloroplast and pyrenoid (initially), mass transfer coefficients were taken from the *Phaeodactylum tricornutum* model and scaled up to fit the larger cell size (20 μm in diameter) of diatom species found in the WAP. Inter-conversion of CO_2 and HCO_3^- within the cell and at the cell surface is catalyzed by carbonic anhydrase. External CA activity was measured in the ambient diatom communities as described above and used in the model. The overall intracellular CA activity was measured for *F. cylindrus* using ^{18}O-exchange (Rost *et al.*, 2003; Hopkinson *et al.*, 2011). The relative distributions of CA among cellular compartments follow that of Hopkinson *et al.* (2011). Although CA activity is high in the cytoplasm and pyrenoid, it is absent from the chloroplast stroma so that HCO_3^- can accumulate. Otherwise HCO_3^- is rapidly converted to CO_2, which diffuses out of the chloroplast membrane. The model is robust to significant changes in CA activity in the cytoplasm and pyrenoid; that is the results are unaffected by increases or up to five-fold decreases. CO_2 is fixed in the pyrenoid by Rubisco (Jenks & Gibbs, 2000). Rubisco kinetics (half-saturation constant for CO_2 (K_C) and turnover rate (k_{cat}^c)) determined for *F. cylindrus* were used in the model, and Rubisco was considered fully active (Young *et al.*, 2014). ^{13}C is fractionated by CA hydration and dehydration based on Paneth & O'Leary (1985). The intrinsic fractionation factor for diatom Rubisco (ε_R) has not been measured, and was instead inferred from relationships between the CO_2 to O_2 specificity Rubisco and ε_R of *P. tricornutum* (Tcherkez *et al.*, 2006; Table S2), although a smaller ε_R has been reported for the form 1D Rubisco for the mesophilic coccolithophorid *Emiliania huxleyi* (Boller *et al.*, 2011). Because isotopic fractionations associated with

diffusion and transport are small they were neglected in the model. Model parameter values are detailed in Table S2.

CO_2 and HCO_3^- fluxes and concentrations are first determined by running the model until it reaches a steady state. Then, using the steady-state fluxes, fractionation factors, and specifying the extracellular CO_2 and HCO_3^- isotopic compositions, the isotopic compositions of CO_2 and HCO_3^- in the cellular compartments can be determined using linear algebra as described in Hopkinson *et al.* (2011).

Results

With the increase in light intensity and ice retreat in early November, phytoplankton biomass, dominated by diatoms (microscopically identified species: e.g. *Corethron* spp., *Thalassiosira* spp., *Fragilariopsis* spp. and *Eucampia* spp.) with diameters of *c.* 20 μm, increased throughout November to a maximum Chl*a* concentration of *c.* 45 μg Chl*a* l^{-1} by early December (Fig. 1a). After the crash of the bloom, phytoplankton biomass became dominated by *Phaeocystis* spp. and cryptophytes and remained low (Chl*a* between 1 and 3 μg l^{-1}) until the end of the season. The one exception to this was a modest second bloom of nanoplankton and diatoms (Chl*a* up to 6 μg l^{-1}) from mid-February to late March. See Fig. S2 and Methods S2 and Goldman *et al.* (2014) for pigment data and phytoplankton community composition. During most of the season the ambient CO_2 concentration remained near saturation (20–30 μM; Fig. 1b), with a major decrease at the peak of bloom (*c.* 6.5 μM on 30 November) and a smaller decrease late in the season (*c.* 17 μM on 8 March).

CO_2 saturation of the phytoplankton community

Short-term carbon fixation experiments with the ambient population yielded low $K_{1/2}$ values with an average of *c.* 4 μM CO_2 before and during the bloom (Figs 1b, S3), followed by higher values afterwards, ranging between 6 and 13 μM CO_2 (Fig. 1b). All of these values are significantly lower than the corresponding ambient CO_2 concentrations (Fig. 1b). Based on our measured C fixation kinetics and ambient CO_2 concentration measurements, we calculate that C fixation was between 80% and 90% CO_2 saturated before and during the early onset of the bloom. The relative CO_2 saturation of C fixation decreased to 65–75% at the peak of the bloom and remained *c.* 70–75% for the rest of the season (Fig. 1c). We note that according to measurements of Rubisco kinetics and abundance, essentially all of the Rubisco in the diatoms must have been active to support measured cellular carbon fixation rates during the bloom (Young *et al.*, 2014).

In order to quantify the CO_2 concentration at the site of fixation by the enzyme Rubisco in the species that dominate carbon fixation, it is necessary to know the half-saturation constant, K_C, of the enzyme for its substrate CO_2 in the ambient phytoplankton population. As shown in a companion study by Young *et al.* (2014), K_C values of Rubisco (from mesophilic and psychrophilic diatoms) measured at 0°C are *c.* 15 μM, lower than the air saturated CO_2 concentration at that temperature. Using

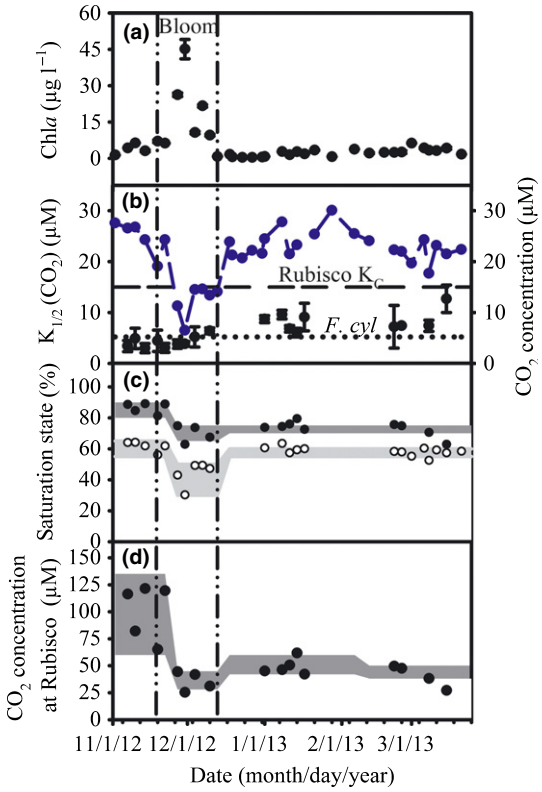

Fig. 1 Biomass and cellular physiology for CO_2 over the summer season 2012/2013 at Palmer Station. (a) Chlorophyll *a* concentration. (b) CO_2 concentration of the bulk seawater (blue dots) and half-saturation concentration of the phytoplankton community (black dots). The horizontal dashed line denotes the measured half-saturation (K_C) of *Fragilariopsis cylindrus* Rubisco extract (Young *et al.*, 2014) and the dotted line indicates the $K_{1/2}$ value measured for *F. cylindrus* cells ($n = 3$). (c) Measured CO_2 saturation of the phytoplankton community (black dots) and range (dark gray area) and calculated CO_2 saturation for Rubisco at bulk seawater CO_2 concentrations (using K_C values of Young *et al.*, 2014) (white dots and light gray shaded area). (d) Calculated CO_2 concentration at the site of Rubisco (black dots). The gray area denoted the calculated range of CO_2 concentrations during the specific time range.

this K_C, we calculate CO_2 concentrations at the site of fixation between 60 and 135 μM during and at the beginning of the bloom, 28–45 μM during the peak of the bloom, and an average of 45 μM afterwards (Fig. 1d). Note that a small change in the percentage carbon saturation results in a large change in calculated substrate concentration and that the results are probably more valid for the bloom period, when diatoms dominated, than afterwards, when other phytoplankton taxa with possibly different K_C for Rubisco (Badger & Andrews, 1987) became important. Nonetheless our results show that the phytoplankton species that dominated carbon fixation during the blooms were able to increase the CO_2 concentration at Rubisco several fold higher (*c.* 3–4-fold) than in the bulk seawater (Fig. 1a,d). This demonstrates the operation of a CCM by the dominant phytoplankton in the bloom community nearly saturating the carboxylating enzyme Rubisco. This process is facilitated by the low temperature, which promotes a high solubility of CO_2 in water and a low half-saturation constant for Rubisco.

HCO_3^- vs CO_2 uptake

The relative contribution of CO_2 and HCO_3^- uptake to cellular inorganic carbon acquisition by the ambient WAP population was measured by $^{14}CO_2$ disequilibrium experiments. The results show that the phytoplankton community used primarily CO_2 as its inorganic carbon source before the spring bloom (Figs 2a, S4). During the peak of the bloom, the community showed more HCO_3^- uptake when the dissolved CO_2 concentration became very low (*c.* 6 μM), with a brief switch back to greater CO_2 usage during an upwelling/mixing event at the peak of the bloom. In the period following the collapse of the spring bloom, phytoplankton cells used mainly CO_2 as their carbon source, whereas in the late season CO_2 and HCO_3^- were both taken up equally (Fig. 2a). Because these data were obtained in the presence of the eCA inhibitor, dextran-bound sulfonamide, they may underestimate the fraction of CO_2 utilized *in situ* if eCA inhibition results in a significant concentration gradient of CO_2 between the bulk medium and the surface of the cells (see Discussion section).

External carbonic anhydrase activity

The activity of eCA was measured by membrane inlet mass spectrometry, MIMS. Measurements with cell suspensions concentrated from field samples demonstrated that the chlorophyll normalized inter-conversion rate between CO_2 and HCO_3^- was increased 10–20-fold above the rate in the absence of cells (Figs 2b, S1; Methods S1) and remained relatively constant throughout the season. We calculate that for a diatom cell of the size of the dominant species during the bloom (*c.* 20 μm diameter), the catalyzed formation of CO_2 from HCO_3^- at the cell surface is *c.* 10 times the CO_2 supply from diffusion (Methods S1).

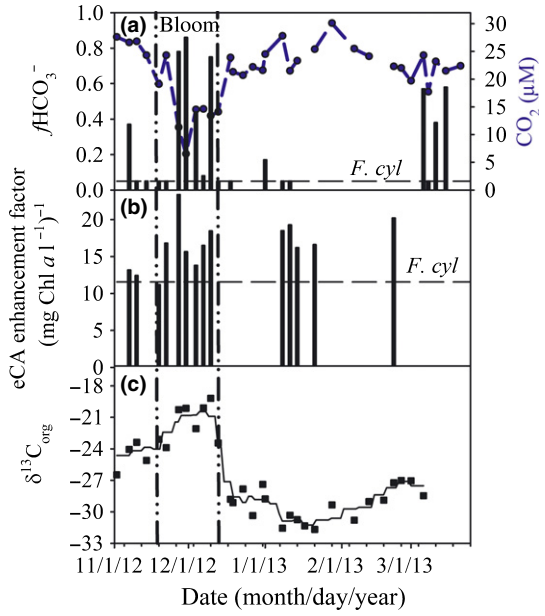

Fig. 2 Measured parameters of CO_2 concentrating mechanism (CCM) activities. (a) Bulk seawater CO_2 concentration (blue dots) and the fraction of HCO_3^- uptake of the phytoplankton community (bars) and *Fragilariopsis cylindrus* (dashed line). (b) Ratio of extracellular carbonic anhydrase (eCA) catalyzed CO_2/HCO_3^- conversion rate over the uncatalyzed CO_2/HCO_3^- conversion rate for the phytoplankton community (bars) and *F. cylindrus* (dashed line). (c) $\delta^{13}C_{org}$ values; line represents the running average of two data points.

Isotopic composition of organic carbon

We also measured the $\delta^{13}C$ of the biomass, $\delta^{13}C_{org}$, a parameter that reflects the overall functioning of the CCM, being affected by the ratio of CO_2 ($\delta^{13}C = -11.1‰$) and HCO_3^- ($\delta^{13}C = 1‰$) taken up and by the exchange of CO_2 between the cell and the external medium, as well as the intrinsic fractionation of Rubisco (Sharkey & Berry, 1985; Schulz *et al.*, 2007). Isotopic analysis of $\delta^{13}C_{org}$ showed strong changes during the season (Fig. 2c). At the beginning of the season, $\delta^{13}C_{org}$ was *c.* −25‰ and increased during the spring bloom, reaching a maximum *c.* −21‰ at the peak. At the crash of the bloom, $\delta^{13}C_{org}$ dropped rapidly, and remained between −28‰ and −32‰ for the rest of the season (Fig. 2c). Such negative values in $\delta^{13}C_{org}$ have been observed in the Southern Ocean region (Goericke & Fry, 1994; Young *et al.*, 2013), but the underlying physiological mechanisms are still under debate.

Laboratory data from *F. cylindrus*

In order to be interpreted quantitatively, our experimental data from the diatom population during the bloom must be integrated into a numerical model of the CCM. But some additional information is necessary to constrain such a model. In particular, as seen in Fig. 3, the CCM of diatoms depends critically on high permeability of membranes to CO_2, but low permeability to HCO_3^-. The CO_2 and HCO_3^- permeability of diatom membranes have been measured in temperate species at 20°C, but could be different at low temperature as the composition of cellular membranes is known to be different in psychrophilic organisms (Morgan-Kiss *et al.*, 2006). We thus performed MIMS experiments, similar to those in Hopkinson *et al.* (2011) to measure the cellular transfer coefficients for CO_2 (f_c) and HCO_3^- (f_b) across the external membrane of *F. cylindrus* at 0°C. Our data show that the cytoplasmic membrane of this psychrophilic organism is highly permeable to CO_2 but essentially impermeable to HCO_3^- (Fig. 4). The calculated transfer coefficients at 0°C for CO_2 (f_c) ~ 2.4×10^{-8} cm^{-3} s^{-1} and for HCO_3^- (f_b) ~ 1.8×10^{-11} cm^{-3} s^{-1} are not significantly different from those obtained in temperate species at 20°C (Hopkinson *et al.*, 2011, 2013).

In the quantitative interpretation of these experiments at low temperature, the boundary layer outside of the cells presents a significant barrier to the diffusion of CO_2, on the same order as the plasmalemma itself. This importance of boundary layer, which results from the two-fold decrease in the diffusion coefficient of CO_2 between 20 and 0°C (Boudreau, 1997), makes our estimation of the membrane permeability to CO_2 relatively imprecise, with a minimal permeability *c.* 10-fold lower than the best estimate (best estimate: 2.4×10^{-1} cm s^{-1}; minimal estimate: 3.7×10^{-2} cm s^{-1}). With the minimal estimate of the

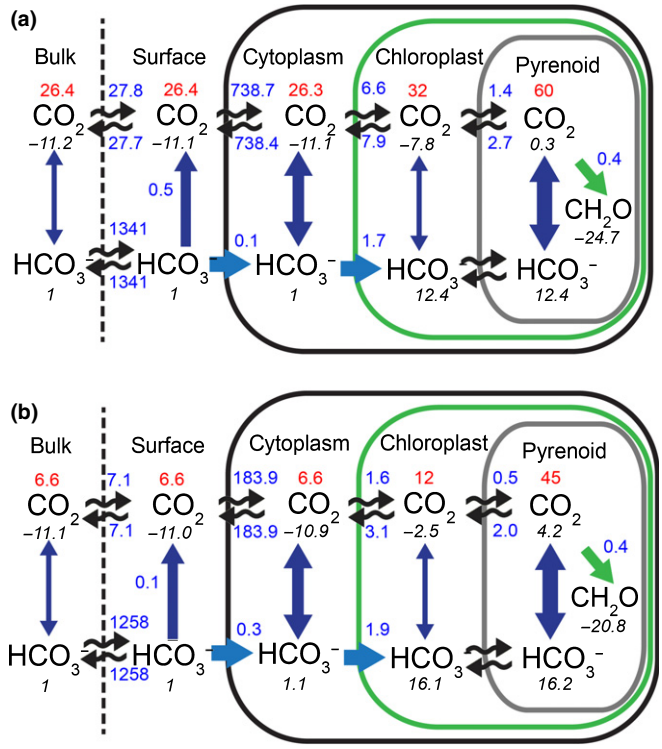

Fig. 3 Results of the carbon isotopic fractionation model for (a) pre-bloom and (b) bloom conditions. The model tracks inorganic carbon concentrations (selected values indicated in red; μM), isotopic composition (italicized in black; ‰), as influenced by inorganic carbon fluxes (blue; $\times 10^{-16}$ mol^{-1} cell^{-1} s^{-1}) and fractionation factors (see the Materials and Methods section). Diffusive fluxes are indicated with wavy arrows, active fluxes are indicated with light blue arrows, and CO_2/HCO_3^- inter-conversion is indicated by dark-blue, double-headed arrows, with thicker arrows denoting rapid, CA-catalyzed inter-conversion and narrow arrows representing slower, spontaneous inter-conversion.

membrane permeability, the boundary layer and the membrane contribute equally to limiting CO_2 fluxes in *F. cylindrus*. However, when scaled up to the larger diatoms found in the WAP and modeled here, the boundary layer resistance is always several-fold more significant, even using the minimal estimate of the membrane permeability. None of the modeling results are affected by the uncertainty in membrane permeability.

Additional experiments with *F. cylindrus* at 1°C, reveal that CO_2 is the major carbon source taken up (Fig. 2a) with a half-saturation constant for carbon fixation ($K_{1/2}$) *c.* 5 μM CO_2 (Fig. 1b). Measured eCA activities normalized to Chl*a* concentrations were similar to those seen in the field data (Figs 2b, S1).

The similar membrane permeability in the psychrophilic diatom compared to the mesophilic diatoms indicates that the membrane permeability of diatoms is neither species nor temperature specific. Similar $K_{1/2}$ values and HCO_3^-/CO_2 uptake ratios observed in diatoms from the WAP and in *F. cylindrus* also indicate that CCM mechanisms are reasonably consistent among psychrophilic diatoms. This provides the justification for the development of a generic CCM model for cold water diatoms.

CCM model for an idealized psychrophilic diatom

We adapted a model for carbon fluxes and carbon isotopic fractionation for the diatom *P. tricornutum* (Hopkinson *et al.*, 2011, 2013) to model large polar diatoms typical of those that dominated the spring bloom during our field studies. A self-consistent model of the CCM was obtained using the parameters obtained experimentally with the field population when available or otherwise with *F. cylindrus* cultures (for model parameters see Table S2).

The need to match the $\delta^{13}C_{org}$ observed during the bloom placed meaningful constraints on uncertain parameters, such as the permeability of the pyrenoid to CO_2. On the one hand, to achieve a *c.* 4‰ decrease in $\delta^{13}C_{org}$ in the course of the bloom (to match observations), the background gross fluxes of CO_2 into and out of the pyrenoid and chloroplast must be a significant fraction of the total fluxes under pre-bloom environmental conditions such that a major drop in these fluxes as extracellular CO_2 declines has a significant effect on $\delta^{13}C_{org}$. This is most readily achieved with a high permeability to CO_2. On the other

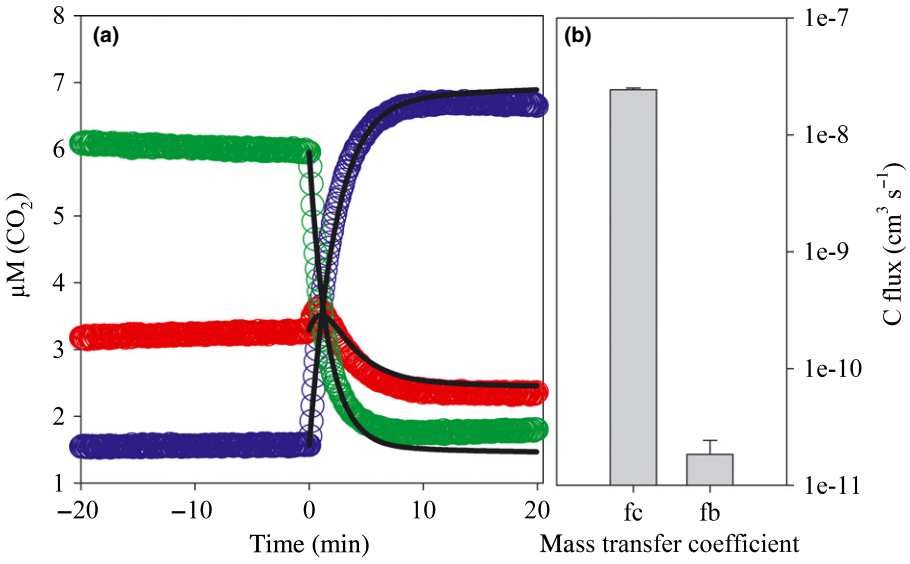

Fig. 4 Membrane permeability of the psychrophilic diatom *Fragilariopsis cylindrus* at 0°C. (a) Model fit (solid black lines) of a single compartment model (described in Hopkinson *et al.*, 2011) to ^{18}O-CO_2 data. Purple circles, $^{13}C^{16}O^{16}O$; red circles, $^{13}C^{16}O^{18}O$; green circles, $^{13}C^{18}O^{18}O$. Cells are added at $t = 0$. (b) Calculated mass transfer coefficients for CO_2 'fc' and HCO_3^- 'fb' for fluxes across the cytoplasmic membrane (according to Hopkinson *et al.*, 2011). Data present mean values ($n = 3$; ± SD).

hand, achieving a high CO_2 concentration in the pyrenoid with a reasonably effective CCM requires a low permeability of the pyrenoid to CO_2, so that an intermediate value must be chosen in the model (Table S2). The modeled HCO_3^- and CO_2 concentrations in various cellular compartments, along with fluxes and isotopic composition are shown in Fig. 3 for the start and peak of the bloom. As can be seen, the increase in $\delta^{13}C_{org}$ during the bloom is properly accounted for.

The model shows that the rate of HCO_3^- transport into the chloroplast and CCM efficiency (defined, for example, as the number of moles of CO_2 fixed per mole of HCO_3^- transported into the chloroplast) remain largely unchanged by environmental conditions. As the extracellular CO_2 decreases during the bloom, the CO_2 concentration in the chloroplast also decreases, keeping the CO_2 gradient between the pyrenoid and bulk seawater constant (Fig. 3). The rate of CO_2 leakage, which determines the efficiency of the CCM and is dependent on this gradient, is also unaffected. The drop in CO_2 in the pyrenoid at the peak of the bloom leads to a slight decrease in photosynthetic rate (6%) as the saturation state of Rubisco declines. Active uptake of HCO_3^- into the chloroplast is the major active carbon flux, the only other active flux being HCO_3^- uptake into the cytoplasm, which is small by comparison. Imprinted on top of the net fluxes driven by active transport are large gross fluxes of CO_2 that result from the high permeability of membranes to CO_2. These gross fluxes are comparable to the net fluxes across the pyrenoid and chloroplast boundaries, and are much greater than active fluxes across the cytoplasmic membrane. CA on the cell surface, in the cytoplasm, and in the pyrenoid serves to keep CO_2 and HCO_3^- concentrations at or near equilibrium.

Discussion

Low temperatures affect several physical, chemical and biochemical processes that are important to the functioning of a CCM in psychrophilic phytoplankton: the CO_2 solubility in seawater increases from *c.* 13 μM at 20°C to *c.* 25 μM at 0°C at equilibrium with the atmosphere; the diffusion coefficient of dissolved CO_2 decreases (by a factor of 2 between 20 and 0°C (Boudreau, 1997)); the affinity of enzymes for their substrate changes (e.g. the K_C of diatom Rubisco decreases from *c.* 50 μM at 20°C to *c.* 15 μM at 0°C (Young *et al.*, 2014)); and the turnover rate of most enzymes decrease (e.g. by a factor of 10 for Rubisco between 20 and 0°C (Young *et al.*, 2014)), although some cold-adapted enzymes maintain relatively high kinetics (as is apparently the case for carbonic anhydrase in the diatoms in the WAP).

CCM activity in the phytoplankton population in the WAP

The existence of a CCM in psychrophilic phytoplankton has been demonstrated in several previous studies (Mitchell & Beardall, 1996; Cassar *et al.*, 2004; Tortell *et al.*, 2008a,b, 2010; Neven *et al.*, 2011; Trimborn *et al.*, 2013). Our results provide additional information on the CCM in phytoplankton communities from the highly productive coastal areas, focusing particularly on an intense spring diatom bloom with CO_2 concentrations falling near 6 μM. Direct evidence for a CCM is given by whole cell $K_{1/2}$ (*c.* 4 μM CO_2 during the bloom in our study) that is lower than the half-saturation constant (K_C) of 15 μM CO_2 for Rubisco at 0°C (Young *et al.*, 2014). The K_C of Rubisco in the ambient population, from which the $K_{1/2}$ values were obtained, may not be exactly equal to that measured in cell extract from laboratory species, but the similar K_C values at 0°C for both *F. cylindrus* and *Thalassiosira weissflogii* observed by Young *et al.* (2014) imply that it is the low temperature that is mostly responsible for the low K_C of the enzyme, rather than a difference in its intrinsic properties among different species (Badger *et al.*, 1998).

The mean $K_{1/2}$ values we measured during the bloom is near values previously measured in the Southern Ocean (Tortell *et al.*, 2010) but slightly higher than previous laboratory data on Southern Ocean diatom cultures (Mitchell & Beardall, 1996; Trimborn *et al.*, 2013). The high degree of saturation of carbon fixation achieved at ambient CO_2 concentrations results from the much higher CO_2 concentration maintained by the CCM at the site of fixation (i.e. Fig. 1c). A degree of saturation *c.* 80–85% is likely near the maximum achievable, as a higher saturation would require the CCM to maintain a much larger CO_2 gradient between Rubisco and the external medium. For example, 90% saturation of the carboxylating enzyme would require a concentration of *c.* 135 μM ($9 \times K_C$), compared to only 60 μM ($4 \times K_C$) for 80% saturation. Because the cytoplasmic concentration must be maintained slightly below that of the seawater (*c.* 20 μM), such an increase would result in nearly a doubling of the leakage of CO_2 from the site of fixation and, hence, roughly two times more energy expended on the CCM (as explained in the last section of the discussion).

The results of our $^{14}CO_2$ disequilibrium experiments show a dominance of CO_2 utilization for most of the season, with a higher HCO_3^- usage at the peak of the bloom. This observation of a switch from CO_2 to HCO_3^- usage in the field is novel. Whereas Tortell *et al.* (2008a,b) found predominant HCO_3^- uptake (> 60%) in the Ross Sea, Cassar *et al.* (2004) and Neven *et al.* (2011) measured a broader range, from primarily CO_2 usage to mostly HCO_3^- usage. In laboratory experiments, Trimborn *et al.* (2013) showed that preferences for an inorganic carbon source are partly species-specific and our data for *F. cylindrus* indicate a preference for CO_2. Neven *et al.* (2011) reported an inverse correlation between HCO_3^- uptake and CO_2 concentration over a small range of CO_2 concentrations, but Cassar *et al.* (2004) and Tortell *et al.* (2010) observed no correlation. A difference between our and other field studies is that we followed the same phytoplankton community over several weeks whereas previous studies compared CCM activity at various sampling sites, where the phytoplankton assemblages as well as environmental conditions were likely different.

The $\delta^{13}C_{org}$ data showed a meaningful shift from relatively light (−25‰) to heavier (−21‰) $\delta^{13}C_{org}$ as the spring bloom developed. Because diatoms dominated the bloom we would expect the intrinsic fractionation by Rubisco to remain nearly constant. Most explanations for shifts in $\delta^{13}C_{org}$ focus on the

source of inorganic carbon (CO_2 or HCO_3^-) and the efficiency of inorganic carbon use (Keller & Morel, 1999; Laws *et al.*, 2002). The shift in inorganic carbon source (Fig. 2a) from the isotopically lighter CO_2 (−11.1‰) to the isotopically heavier HCO_3^- (+1‰) could, in principle, explain the $\delta^{13}C_{org}$ decrease from *c.* −25‰ to −21‰ during the bloom as the fraction of HCO_3^- usage ranges from *c.* 0 to 0.9. However, other explanations are possible and discussed below.

After the bloom, the $\delta^{13}C_{org}$ became very light (−30‰), and remained light for the rest of the season. This could have resulted from a slower growth rate, which would allow for a fuller expression of the isotopic discrimination by Rubisco. For example, Tortell *et al.* (2013) found the isotopic composition to be strongly positively correlated to the ratio of growth rate and CO_2 concentration. But this effect is not likely to fully explain the low $\delta^{13}C_{org}$ we observed after the diatom bloom as the CO_2 concentration stayed near saturation and data on primary production (based on either oxygen evolution or carbon fixation rates) normalized to Chl*a* imply that phytoplankton growth rates remained high (Goldman *et al.*, 2014). The very negative $\delta^{13}C_{org}$ observed in the late season thus results likely in part from the dominance of new phytoplankton taxa including cryptophytes and *Phaeocystis* (Fig. S2 and Goldman *et al.*, 2014) with a carbon acquisition and fixation machinery somewhat different from that operating during the bloom.

Insights from a CCM model for an idealized psychrophilic diatom

Our numerical model was used to explore the role of eCA and extracellular HCO_3^- uptake in the functioning of the CCM in psychrophilic phytoplankton, as well as to explore the reason for the observed shift in $\delta^{13}C_{org}$ during the diatom bloom.

It is generally assumed that the primary role of eCAs is to facilitate CO_2 influx by maintaining a high CO_2 concentration at the cell surface (Moroney *et al.*, 1985; Elzenga *et al.*, 2000). This could be particular important for polar diatoms during bloom situations, as the supply of CO_2 by diffusion from the bulk is reduced by the low diffusion coefficient and the large size of the organisms. However, if eCA is eliminated from the model, the bulk to surface CO_2 gradient is 0.5 μM under pre-bloom conditions, when CO_2 uptake dominates, but only 0.1 μM under bloom conditions, when HCO_3^- uptake dominates. These gradients are quite small and the benefit of eCA activity seems modest as the inward CO_2 flux could be maintained by a small increase in the rate of HCO_3^- transport into the chloroplast. Previous studies have shown that eCA is only critical for photosynthesis when CO_2 concentration are very low, but have suggested that there is a small energetic benefit from eCA obtained from reducing the extent to which CO_2 needs to be drawn-down in the cytoplasm to foster diffusive CO_2 uptake (Burkhardt *et al.*, 2001; Hopkinson *et al.*, 2013).

Similarly, the energetic benefit of switching from CO_2 to HCO_3^- uptake during the bloom is not obvious. The high rates of eCA activity would allow continued high rates of CO_2 uptake even at the low CO_2 concentrations during the bloom. In the model, CO_2 uptake is energetically cheaper than HCO_3^- uptake because it is ultimately driven by HCO_3^- transport from the cytoplasm to the chloroplast, which must be done anyway.

Our model of the CCM offers a novel explanation for the shift from relatively light to heavier $\delta^{13}C_{org}$ as the diatom bloom developed. In our model the shift in the inorganic carbon source on its own causes a less than 0.5‰ change in $\delta^{13}C_{org}$. Instead it is the decrease in external CO_2 concentration that causes the majority of the increase in $\delta^{13}C_{org}$. Because the cell membranes are highly permeable to CO_2, the large gross fluxes of CO_2 into and out of the cellular compartments reduce intracellular $\delta^{13}C$-CO_2 accumulation (Fig. 3). These fluxes, especially with the high CO_2 concentrations in the pre-bloom period, are comparable to the net carbon fluxes actively driven by the CCM and have a major effect on the isotopic composition of intracellular inorganic carbon but are not directly related to CCM activity or efficiency. As the CO_2 concentration declines during the bloom the gross cellular CO_2 fluxes are significantly reduced leading to heavier $\delta^{13}C$-CO_2 in the chloroplast and correspondingly heavier $\delta^{13}C_{org}$. The presence of these gross background fluxes also explains why the shift in inorganic carbon source from CO_2 to HCO_3^- has so little effect on $\delta^{13}C_{org}$ bringing in isotopically light CO_2 that is mixed with intracellular HCO_3^- via CA activity to keep the isotopic composition of inorganic carbon species in the cytoplasm very close to external values regardless of the inorganic carbon source (e.g. Fig. 3).

Finally, our numerical model provides the means to explore how the various effects of low temperature influence the CCM of psychrophilic phytoplankton and consequently the energetics of the cells. The high solubility of CO_2 and the low K_C of Rubisco at low temperatures greatly decrease the concentration gradient that must be maintained by the CCM between the site of fixation and the bulk solution to nearly saturate the carboxylation reaction. For example, at 0°C, 80% saturation of Rubisco is achieved at a CO_2 concentration of 60 μM, compared to an atmospheric equilibrium concentration of 25 μM; at 20°C, these numbers become 150 and 13 μM, respectively. The net result is a much smaller CO_2 diffusive flux from the site of fixation to the cytoplasm at low temperature, and hence a much smaller ratio of inorganic carbon transported across membranes to carbon fixed: from 4 at 0°C to 14 at 20°C (obtained by running the same model with the appropriate change in parameters). The corresponding savings are on the order of five ATP per molecule of CO_2 fixed or *c.* 250 kJ mol^{-1} CO_2 fixed, assuming that SLC4 type transporters found in other diatoms are used with an energetic cost of 0.5 ATP per HCO_3^- transported (Hopkinson *et al.*, 2011; Nakajima *et al.*, 2013). This energy saving is substantial compared with the 590 kJ mol^{-1} required to reduce carbon in the Calvin-Benson cycle (3 ATP + 2 NADPH; Falkowski & Raven, 2007). The energy costs for the CCM are higher than values presented in Raven *et al.* (2014), which assumed low leakage rates to determine minimal costs of the CCM, whereas leakage is several times the rate of CO_2 fixation in our model.

Altogether, our results show that the CCM of diatoms that dominated carbon fixation during the spring bloom we observed in the WAP is able to nearly saturate Rubisco. Such near

saturation of carbon fixation is particularly important in cold water as the turnover rate of the enzyme decreases, necessitating a large increase in cellular Rubisco concentration (Young *et al.*, 2014). Fortunately, as we have shown, the lower temperature also decreases markedly the energy required to achieve saturation of the carboxylating enzyme. This is due principally to the smaller K_C of Rubisco (Young *et al.*, 2014) and secondarily to the higher solubility of CO_2 in cold water.

Acknowledgements

We wish to acknowledge the exceptional assistance provided by the science support and administrative staff at Palmer Station and the entire Palmer LTER science team. We also want to acknowledge the help Björn Rost and Jana Hölscher (AWI, Germany) for the help with the analysis of total alkalinity samples. This study was supported by funds from the US National Science Foundation (OPP 1043593, EF 1040965, OCE 0825192); B.M.H. was supported by funds from the US National Science Foundation (EF 1041034, MCB 1129326); P.D.T. was supported by the Natural Sciences and Engineering Research Council (NSERC) Canada.

References

Arrigo KR, van Dijken GL, Bushinsky S. 2008b. Primary production in the Southern Ocean, 1997–2006. *Journal of Geophysical Research-Oceans* **113**: C08004. doi: 10.1029/2007jc004551.

Arrigo KR, van Dijken G, Long M. 2008a. Coastal Southern Ocean: a strong anthropogenic CO_2 sink. *Geophysical Research Letters* **35**: L21602. doi: 10.1029/2008gl035624.

Badger MR, Andrews TJ. 1987. Co-evolution of Rubisco and CO_2 concentrating mechanisms. In: Biggins J, ed. *Progress in photosynthesis research.* Proceedings of the VIIth International Congress on Photosynthesis, Providence, Rhode Island, USA. Dordrecht, the Netherlands: Martinus Nijhoff Publishers, 601–609.

Badger MR, Andrews TJ, Whitney SM, Ludwig M, Yellowlees DC. 1998. The diversity and co-evolution of Rubisco, plastids, pyrenoids and chloroplast-based CO_2-concentrating mechanisms in the algae. *Canadian Journal of Botany* **76**: 1052–1071.

Becker DA. 1990. Homogeneity and evaluation of the New Nist leaf certified reference materials. *Biological Trace Element Research* **26–7**: 571–577.

Boller AJ, Thomas PJ, Cavanaugh CM, Scott KM. 2011. Low stable carbon isotope fractionation by coccolithophore RubisCO. *Geochimica et Cosmochimica Acta* **75**: 7200–7207.

Boudreau BP. 1997. *Diagenetic models and their implementation modelling transport and reactions in aquatic sediments.* Berlin, Germany: Springer.

Brewer PG, Bradshaw AL, Williams RT. 1986. Measurements of total carbon dioxide and alkalinity in the North Atlantic Ocean. In: Trabalka JR, Reichle DE, eds. *The changing carbon cycle: a global analysis.* New York, NY, USA: Springer, 348–370.

Burkhardt S, Amoroso G, Riebesell U, Sültemeyer D. 2001. CO_2 and HCO_3^- uptake in marine diatoms acclimated to different CO_2 concentrations. *Limnology and Oceanography* **46**: 1378–1391.

Cassar N, Laws EA, Bidigare RR, Popp BN. 2004. Bicarbonate uptake by Southern Ocean phytoplankton. *Global Biogeochemical Cycles* **18**: GB2003. doi: 10.1029/2003gb002116.

Dickson AG, Millero FJ. 1987. A comparison of the equilibrium constants for the dissociation of carbonic acid in seawater media. *Deep Sea Research* **34**: 1733–1743.

Dutkiewicz S, Follows MJ, Bragg JG. 2009. Modeling the coupling of ocean ecology and biogeochemistry. *Global Biogeochemical Cycles* **23**: GB4017. doi: 10.1029/2008GB003405.

Egleston ES, Sabine CL, Morel FMM. 2010. Revelle revisited: buffer factors that quantify the response of ocean chemistry to changes in DIC and alkalinity. *Global Biogeochemical Cycles* **24**: GB1002. doi: 10.1029/2008gb003407.

Elzenga JTM, Prins HBA, Stefels J. 2000. The role of extracellular carbonic anhydrase activity in inorganic carbon utilization of *Phaeocystis globosa* (Prymnesiophyceae): a comparison with other marine algae using the isotopic disequilibrium technique. *Limnology and Oceanography* **45**: 372–380.

Espie GS, Colman B. 1986. Inorganic carbon uptake during photosynthesis: 1: a theoretical-analysis using the isotopic disequilibrium technique. *Plant Physiology* **80**: 863–869.

Falkowski PG, Raven JA. 2007. *Aquatic photosynthesis.* Oxford, UK: Blackwell Publishers.

Giordano M, Beardall J, Raven JA. 2005. CO_2 concentrating mechanisms in algae: mechanisms, environmental modulation, and evolution. *Annual Review of Plant Biology* **56**: 99–131.

Goericke R, Fry B. 1994. Variations of marine plankton $\delta^{13}C$ with latitude, temperature, and dissolved CO_2 in the world ocean. *Global Biogeochemical Cycles* **8**: 85–90.

Goldman JAL, Kranz SA, Young JN, Tortell PD, Stanley RHR, Bender ML, Morel FMM. 2014. Gross and net production during the spring bloom along the Western Antarctic Peninsula. *New Phytologist* **205**: 182–191.

Gran G. 1952. Determination of the equivalence point in potentiometric titrations. Part II. *The Analyst* **77**: 661–671.

Holm-Hansen O, Mitchell BG, Hewes CD, Karl DM. 1989. Phytoplankton blooms in the vicinity of Palmer Station, Antarctica. *Polar Biology* **10**: 49–57.

Hopkinson BM, Dupont CL, Allen AE, Morel FMM. 2011. Efficiency of the CO_2-concentrating mechanism of diatoms. *Proceedings of the National Academy of Sciences, USA* **108**: 3830–3837.

Hopkinson BM, Meile C, Shen C. 2013. Quantification of extracellular carbonic anhydrase activity in two marine diatoms and investigation of its role. *Plant Physiology* **162**: 1142–1152.

Jenks A, Gibbs SP. 2000. Immunolocalization and distribution of Form II Rubisco in the pyrenoid and chloroplast stroma of *Amphidinium carterae* and Form I Rubisco in the symbiont-derived plastids of *Peridinium foliaceum* (Dinophyceae). *Journal of Phycology* **36**: 127–138.

Keller K, Morel FMM. 1999. A model of carbon isotopic fractionation and active carbon uptake in phytoplankton. *Marine Ecology Progress Series* **182**: 295–298.

Laws EA, Popp BN, Cassar N, Tanimoto J. 2002. ^{13}C discrimination patterns in oceanic phytoplankton: likely influence of CO_2 concentrating mechanisms, and implications for palaeoreconstructions. *Functional Plant Biology* **29**: 323–333.

Lewis E, Wallace DWR. 1998. Program developed for CO_2 system calculations. ORNL/CDIAC-105: (Carbon Dioxide Information Analysis Center, Oak Ridge National Laboratory, US Department of Energy, Oak Ridge, Tennesse, 1998).

Martin CL, Tortell PD. 2006. Bicarbonate transport and extracellular carbonic anhydrase activity in Bering Sea phytoplankton assemblages: results from isotope disequilibrium experiments. *Limnology and Oceanography* **51**: 2111–2121.

Mehrbach C, Culberson CH, Hawley JE, Pytkowicz RM. 1973. Measurement of the apparent dissociation constants of carbonic acid in seawater at atmospheric pressure. *Limnology and Oceanography* **18**: 897–907.

Mitchell C, Beardall J. 1996. Inorganic carbon uptake by an Antarctic sea-ice diatom *Nitzchia frigida. Polar Biology* **16**: 95–99.

Morgan-Kiss RM, Priscu JC, Pocock T, Gudynaite-Savitch L, Huner NP. 2006. Adaptation and acclimation of photosynthetic microorganisms to permanently cold environments. *Microbiology and Molecular Biology Reviews* **70**: 222–252.

Moroney JV, Husic HD, Tolbert NE. 1985. Effect of carbonic-anhydrase inhibitors on inorganic carbon accumulation by *Chlamydomonas reinhardtii. Plant Physiology* **79**: 177–183.

Nakajima K, Tanaka A, Matsuda Y. 2013. SLC4 family transporters in a marine diatom directly pump bicarbonate from seawater. *Proceedings of the National Academy of Sciences, USA* **110**: 1767–1772.

Neven IA, Stefels J, van Heuven SMAC, de Baar HJW, Elzenga JTM. 2011. High plasticity in inorganic carbon uptake by Southern Ocean phytoplankton

in response to ambient CO_2. *Deep-Sea Research Part II-Topical Studies in Oceanography* **58**: 2636–2646.

Paneth P, Oleary MH. 1985. Carbon isotope effect on dehydration of bicarbonate ion catalyzed by carbonic-anhydrase. *Biochemistry* **24**: 5143–5147.

Raven JA, Beardall J, Giordano M. 2014. Energy costs of carbon dioxide concentrating mechanisms in aquatic organisms. *Photosynthesis Research* **121**: 111–124.

Rost B, Kranz SA, Richter K-U, Tortell PD. 2007. Isotope disequilibrium and mass spectrometric studies of inorganic carbon acquisition by phytoplankton. *Limnology and Oceanography Methods* **5**: 328–337.

Rost B, Riebesell U, Burkhardt S, Sueltemeyer D. 2003. Carbon acquisition of bloom-forming marine phytoplankton. *Limnology and Oceanography* **48**: 55–67.

Schulz KG, Rost B, Burkhardt S, Riebesell U, Thoms S, Wolf-Gladrow DA. 2007. The effect of iron availability on the regulation of inorganic carbon acquisition in the coccolithophore *Emiliania huxleyi* and the significance of cellular compartmentation for stable carbon isotope fractionation. *Geochimica et Cosmochimica Acta* **71**: 5301–5312.

Sharkey TD, Berry JA. 1985. Carbon isotope fractionation of algae influenced by an inducible CO_2-concentrating mechanism. In: Lucas WJ, Berry JA, eds. *Inorganic carbon uptake by aquatic photosynthetic organisms*. Rockville, RI, USA: American Society of Plant Physiologists, 389–401.

Silverman DN. 1982. Carbonic-anhydrase – O-18 exchange catalyzed by an enzyme with rate-contributing proton-transfer steps. *Methods in Enzymology* **87**: 732–752.

Smetacek V, Scharek R, Gordon LI, Eicken H, Fahrbach E, Rohardt G, Moore S. 1992. Early spring phytoplankton blooms in ice platelet layers of the Southern Weddell Sea, Antarctica. *Deep-Sea Research Part A-Oceanographic Research Papers* **39**: 153–168.

Sullivan CW, Arrigo KR, Mcclain CR, Comiso JC, Firestone J. 1993. Distributions of phytoplankton blooms in the Southern Ocean. *Science* **262**: 1832–1837.

Sunda WG, Price NM, Morel FMM. 2005. Trace metal ion buffers and their use in culture studies. In: Andersen RA, ed. *Algal culturing techniques*. Amsterdam, the Netherlands: Elsevier, 35–63.

Sweeney C. 2003. The annual cycle of surface water CO_2 and O_2 in the Ross Sea. In: Dunbar RB, DiTullio GR, eds. *Biogeochemistry of the Ross Sea*. Washington, DC, USA: AGU, 295–312.

Tcherkez GGB, Farquhar GD, Andrews TJ. 2006. Despite slow catalysis and confused substrate specificity, all ribulose bisphosphate carboxylases may be nearly perfectly optimized. *Proceedings of the National Academy of Sciences, USA* **103**: 7246–7251.

Tortell PD, Mills MM, Payne CD, Maldonado MT, Chierici M, Fransson A, Alderkamp AC, Arrigo KR. 2013. Inorganic C utilization and C isotope fractionation by pelagic and sea ice algal assemblages along the Antarctic continental shelf. *Marine Ecology Progress Series* **483**: 47–66.

Tortell PD, Payne C, Gueguen C, Strzepek RF, Boyd PW, Rost B. 2008a. Inorganic carbon uptake by Southern Ocean phytoplankton. *Limnology and Oceanography* **53**: 1266–1278.

Tortell PD, Payne CD, Li YY, Trimborn S, Rost B, Smith WO, Riesselman C, Dunbar RB, Sedwick P, DiTullio GR. 2008b. CO_2 sensitivity of Southern Ocean phytoplankton. *Geophysical Research Letters* **35**: L04605. doi: 10.1029/2007gl032583.

Tortell PD, Trimborn S, Li YY, Rost B, Payne CD. 2010. Inorganic carbon utilization by Ross Sea phytoplankton across natural and experimental CO_2 gradients. *Journal of Phycology* **46**: 433–443.

Trimborn S, Brenneis T, Sweet E, Rost B. 2013. Sensitivity of Antarctic phytoplankton species to ocean acidification: growth, carbon acquisition, and species interaction. *Limnology and Oceanography* **58**: 997–1007.

Welschmeyer NA. 1994. Fluorometric analysis of chlorophyll-a in the presence of chlorophyll-b and pheopigments. *Limnology and Oceanography* **39**: 1985–1992.

Young JN, Bruggeman J, Rickaby REM, Erez J, Conte M. 2013. Evidence for changes in carbon isotopic fractionation by phytoplankton between 1960 and 2010. *Global Biogeochemical Cycles* **27**: 505–515.

Young JN, Goldman JAL, Kranz SA, Tortell PD, Morel FMM. 2014. Slow carboxylation of Rubisco constrains the maximum rate of carbon fixation during Antarctic phytoplankton blooms. *New Phytologist* **205**: 172–181.

Zeebe RE, Wolf-Gladrow DA. 2007. *CO_2 in seawater: equilibrium, kinetics, isotopes*. Amsterdam, the Netherlands: Elsevier Science B.V.

Zhang HN, Byrne RH. 1996. Spectrophotometric pH measurements of surface seawater at *in situ* conditions: absorbance and protonation behavior of thymol blue. *Marine Chemistry* **52**: 17–25.

Supporting Information

Additional supporting information may be found in the online version of this article.

Fig. S1 Raw data of a representative mass spectrometric CA assay.

Fig. S2 Pigments data and phytoplankton species composition for major taxa.

Fig. S3 Michaelis–Menten fits to determine the $K_{1/2}$ values and to calculate the CO_2 saturation of the phytoplankton community.

Fig. S4 ^{14}C disequilibrium raw data and model fits.

Table S1 Environmental parameters

Table S2 Model parameter values

Methods S1 Analysis of pigment composition for Fig. S2.

Methods S2 External carbonic anhydrase activity.

Please note: Wiley Blackwell are not responsible for the content or functionality of any supporting information supplied by the authors. Any queries (other than missing material) should be directed to the *New Phytologist* Central Office.